Simultaneous Bending and Torsion Deflection Measurement of Flexible Robotic Link Using Position Sensing Detectors

G. Balyasin*, G. Liu*, W. Zhu**

* Department of Aerospace Engineering, Ryerson University, Toronto, Canada
george.balyasin@ryerson.ca; gjliu@ryerson.ca

** Space Exploration, Canadian Space Agency, Canada
Wen-Hong.Zhu@asc-csa.gc.ca

Abstract

It is well known that flexibility of robotic links causes deformation and reduced positioning accuracy of the robot at the end-effector and this problem becomes more complicated when the links are made of new materials such as composite. Various approaches including strain gauges, fiber Bragg grating, computer vision and optoelectronics have been applied to solve the problem. This paper proposes an optoelectronic method with a reduced number of position sensing detectors and laser diodes to determine both bending and torsion deformations of a robotic link. The attachment of two optoelectronic sensors on the link and two laser dots produced on these sensors by lasers provide the data required for computations and the tip deflection values are obtained by trigonometric functions along with iterative computations. The method has been analysed to identify possible sources of error. Experiments were conducted to verify the proposed method and the results have demonstrated its efficiency.

1 Introduction

Space robotic manipulators are involved in on-orbit missions including handling of modules during construction of International Space Station and subsequent station repairs, as well as capturing and redeployment of satellites when in need of repairs and now potentially refueling. The robotic activities may require work with high positioning accuracy. It is well known that applied loads and momentum cause the deformation of flexible robotic links, thus leading to positioning errors. There is need to measure the error introduced by the link deformation in order to guide the robotic device manipulators to the intended position after error compensation. The main task of the present work is to measure both bending and torsion deformations of a robotic link accurately (submillimeter scale) with position sensing detectors and lasers.

The known approaches to detect flexible link deformation use either optics, strain gauges, fiber or computer vision. To determine deformation using light, [1] proposed a method where fiber Bragg grating is used to filter out wavelengths of light out of optical fiber based on the stress the fiber experienced at sensor location. Thus having a number of such sensors scattered along a robotic link would, in combination with stress analysis theory, predict and estimate its deformation.

In [2], a camera used to track the centres of two spheres attached to and moving with the link's end-effector provides deflection data by noting the difference between expected and observed sphere positions. For [3], the results were available for both bending and torsion, however, for methods where camera is used nothing can get in between camera and the marker/s. To keep the image resolution good enough to detect deflection on millimeter scale and torsion of 1-2 degrees, the camera can't be too far from the link. Also, camera sampling rate has to be adequate to supply image data of sufficient resolution, at least every few milliseconds. Since a multi-link manipulator will have to be entirely within camera's field of view, the link's possible length is limited.

A common method of determining beam deflection is through analysis of signals coming from strain gauges strategically placed along the length of a link as described in [4] and [3]. As load is applied to the link, the resulting strain measurements combined with an accurate mathematical link model allow the prediction of link's deformed shape. While knowing the total amount of deflection it is then possible to deduct or extrapolate the link-tip's new location. The strain gauge method provides both bending and torsion information. The acquired beam torsion values from gauges can be extrapolated and thus indirectly indicate the tip's angle of twist.

Groups of strain gauges combined into load cells can be installed on a robotic link, however, there will be a need of gauges calibration for thermal expansion of material due to their thermal sensitivity and the wide temperature range encountered in space environment, even if no load is present. To attach strain gauges directly on a link, the area of application has to be clean; if glue is used it has to last for the duration of gauge use. The longer the robotic link is the longer the wires running from gauge to monitoring system are, which will affect the readings. Using a wireless gauge monitoring system instead, will lead to extra hardware and costs. Finally, strain gauges have certain limitation of the strain they can be subjected to, meaning that the loads applied to the robotic link may be limited to predetermined values.

An image processing method used in [4] compared deformation data using strain gauges on a link to a secondary system of infrared markers placed on link's both ends and monitored by an infrared camera.

The general concept behind optoelectronic method is to first have a laser dot shine on the centre of a Position Sensing Detector (PSD) when the link is considered not under load and noting the dot's initial position, then noting the dot location again after a load is applied to the link and its tip moved from initial position to a different position. The laser dots that once were on the centers of PSDs move on the sensor surface in proportion to the tip deformation.

In [5] and [6], a setup of 3 PSDs and 3 laser diodes is introduced to measure the translation of the link's tip in the plane of the PSDs, and a mathematical method is provided for calculating the link's twist. In [7], a single PSD and a laser diode were used to detect the vibration of a moving link's tip and its damping, all in one dimension. Articles [8] and [9] describe the use of a single PSD to determine the deflection of a coordinate measuring arm. Here the measured deflection is in the X and Y axes of a coordinate system with Z axes parallel to the laser beam which shines from one end of link to the other. Link torsion was not considered. However, a list of sources of deformation is provided - among the most considerable sources are the flexible link's own weight, operator's force applied externally on the link, contact force between the link's tip and a surface. Among the experimental errors listed were joint run-outs and encoder errors.

Prisms to split laser beams were used along with PSDs in [10] [11] and [12] to determine end effector positioning errors when the manipulator has more than one link. The deflection of individual links is combined into the overall error magnitude.

Using PSD's may overcome some of the strain gauges' drawbacks. Unlike strain gauge system which processes electric resistance the PSDs process photovoltaics. The laser beams used do not need a medium to travel through and are not affected by electromagnetic field. Attachment of system parts is done at the link ends leading to easy parts replacement, if required. Lastly, the maximum link load that PSD system can operate at is determined by the physical size of the sensors so the laser dots will remain on the sensors' photovoltaic surface during tip deflection.

This paper proposes a link tip movement tracking method that involves just two PSDs installed on a link. Compared to the previously reported approaches, the elimination of a third PSD means not only simpler design with reduced hardware, but also physical space required for the sensor system implementation is reduced along with the overall weight. Also, the method works regardless of laser dots' initial coordinates on the sensors. A robotic arm typically consists of a number of links thus to obtain the end-effector's real current position, as in [10]-[12] for example, the proposed method's measurements of individual link deflections can be combined.

The paper consists of four sections. Section 2 outlines the operation of the PSDs and the description of the proposed deflection measurement method with error source analysis. Section 3 describes the experimental setup, and the experimental results in comparison with that obtained with a vision-based method. Section 4 provides concluding remarks.

2 Bending and Torsion Measurement Method

2.1 Optoelectronics principles

Position Sensing Detector (PSD) is an optoelectronic sensor with one surface that can capture the energy of a laser ray falling on it and then generate an electric current. Sending the generated current from PSD to an amplifier will result in an analog signal being generated which can then be linearly interpreted as position away from the PSD photosensitive surface centre. In a 2-D PSD, two signals will be generated, proportional to the laser dot's position along the sensor's X and Y axes. If the laser dot falls exactly onto the photosensitive surface centre both analog coordinate signals are 0 Volt (without signal noise effects); moving the dot away from the centre will result in generating analog signals respective to the position. The sensor has a specific range of +/- V Volts for each signal and when maximum voltage is generated it means that the laser dot centre is on the sensitive surface's edge. Just like in Cartesian coordinate system, positive voltage means that the X or Y coordinate of the laser dot is positive, opposite with negative voltage.

Total power of laser beam shining on the PSD must be limited in order not to saturate the sensor, and the power density cannot exceed the maximum magnitude

specified in W/cm^2. The variation of laser beam intensity when the laser dots are on the PSD sensitive surface does not affect the reading due to the method of wiring of the four terminals attached to it. Also, the diameter and profile shape of the laser dot on the surface do not affect the readings, provided the beam section is small enough to fit completely on the surface.

2.2 Proposed method of measurement

Fig. 1 defines the frames of reference used in presenting the proposed method. The fixed-end global frame has an origin at the link's fixed-end centroid and is static. The axes X_F and Y_F form a plane perpendicular to the undeformed link, while axis Z_F is perpendicular to that plane. The deflecting tip frame has its origin, and is free to translate with the link's tip centroid, however the axes X_T, Y_T, Z_T always stay parallel to the respective axes of the fixed-end frame. The three measurements required in this study are the link's tip deflection in the global frame's X_F and Y_F axes, as well as the link's torsional angular deflection around the link tip Z_T axis. At zero deformation the tip plane X_T-Y_T on which the photosensitive elements are secured is parallel to the global X_F -Y_F plane; if there is link deformation, the tip and global X-Y planes are no longer in parallel yet assumed to be so. When the system is on and operational, each of the two stationary laser diodes produces a small dot on the corresponding PSD surface. The outer tip of the link under load will move from its original position into some other position corresponding to the magnitude and direction of the acting force. Now the laser dots will no longer be at respective initial positions on the PSD surfaces, but instead settle in other locations.

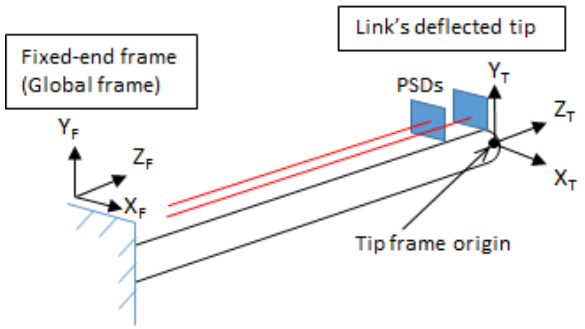

Fig. 1. System setup concept with definition of coordinate system

Based on the signal generated by the PSD-amplifier combination, each PSD will output an analog X/Y coordinate of where on its photosensitive surface is the corresponding laser dot located now, in form of voltage, changing proportionally to dots' movement. A change of 1 Volt in amplified signal corresponds to an established distance of dot movement on the surface along an axis. Knowing the coordinates of two points relative to the link's cross section centre (origin of the tip reference X_T-Y_T frame), the link's twist can be calculated, in part with help of torsion angle iterations.

Fig. 2 depicts all the values computed for one of the two PSDs and the same values are needed for the second PSD. Important to note that the subscript "i" used in this paper represents the fact that similar calculations are done for both PSDs, thus i=1 and i=2.

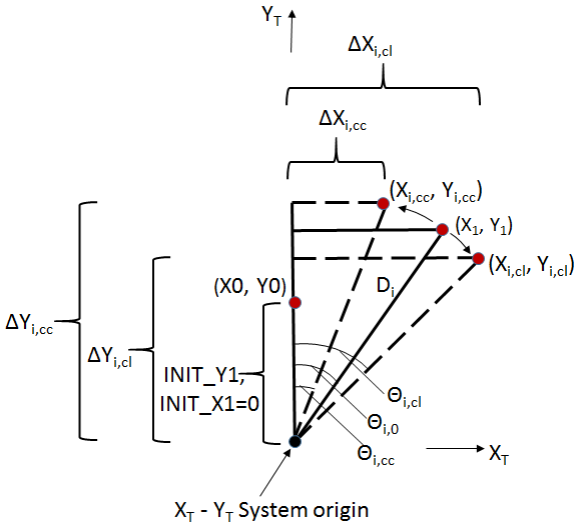

Fig. 2. Depiction of distance components and dot location for rotation angle

The distance between the X_T-Y_T frame origin and the individual PSD centre is measured at time of system installation (Fig. 3); H_i and V_i, are respectively the distance components along the X_T and Y_T axes. The variables $Px_{i,0}$ and $Py_{i,0}$ are the initial (pre-deformation) coordinates of the laser dot on the sensor surfaces given directly by the PSDs (Fig. 3).

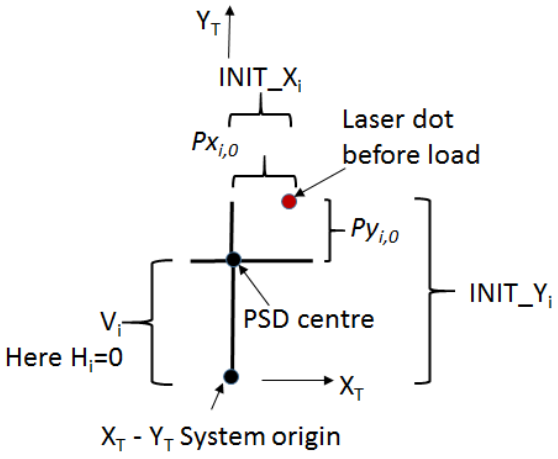

Fig. 3. Position of laser dot before load relative to PSD centre and X_T-Y_T tip frame origin

Before any link deformation occurred, coordinates of each laser dot on corresponding PSD's photosensitive surface are registered and stored. The distances along X_T and Y_T axes, between the dots and tip reference frame origin are obtained through (1) and (2) and called INIT_X_1, INIT_Y_1, INIT_X_2 and INIT_Y_2, respectively for each PSD (Fig. 2).

$$\text{INIT\_X}_i = H_i + Px_{i,0} \quad (1)$$
$$\text{INIT\_Y}_i = V_i + Py_{i,0} \quad (2)$$

As link deformation occurs, the laser dots' coordinates on PSD surfaces (Px_i and Py_i) are registered, thus a new set of distances between dots and tip origin point, called X_1, Y_1 for PSD 1 (Fig. 2) and X_2 and Y_2 for PSD 2 , are found as

$$X_i = H_i + Px_i \quad (3)$$
$$Y_i = V_i + Py_i \quad (4)$$

D_i is the magnitude of the straight line joining X_T-Y_T frame tip origin and the laser dot after deformation, (5).

$$D_i = \sqrt{{X_i}^2 - {Y_i}^2} \quad (5)$$

$\theta_{i,0}$ is the angle the vector D_i makes with an axis of X_T-Y_T frame on which the centre of the i-th PSD lies. The change in each dot's coordinate due to deflection along the two axes gives the tip displacement along those (ΔX and ΔY) and is calculated using (6) and (7),

$$\Delta X_i = \text{INIT\_X}_i - X_i \quad (6)$$
$$\Delta Y_i = \text{INIT\_Y}_i - Y_i \quad (7)$$

If there was no link twist and only bending (Fig. 4b) then a difference between initial and current dot-to-origin distances will be the same for both PSDs using equations (8) and (9), and ΔX_i , ΔY_i would become the tip deflection values.

$$\text{INIT\_X}_1 - X_1 = \text{INIT\_X}_2 - X_2 \quad (8)$$
$$\text{INIT\_Y}_1 - Y_1 = \text{INIT\_Y}_2 - Y_2 \quad (9)$$

If however, the link has experienced torsion along with bending then equations (8) and (9) will not hold.

Since the total deformation consists of bending and twist, computational iterations can be used in order to deduct the twist. The deduction is done by assuming that the laser dots (X_i , Y_i), as they are, are gradually rotated (arbitrary angular resolution) on a circumference (Fig. 2) of a circle with radius D_i that is equal to the current corresponding dot-to-origin distance.

This yields two new angles: $\theta_{i,cc}$ if the rotation of dot position is counter-clockwise (cc), meaning the link rotated counter-clockwise if looked at from laser source and $\theta_{i,cl}$ if dots rotated clockwise (cl), implying the link rotated clockwise.

Using $\theta_{i,cc}$ and $\theta_{i,cl}$, two new triangles (Fig. 2) are constructed on which points with coordinates ($X_{i,cc}$, $Y_{i,cc}$) and ($X_{i,cl}$, $Y_{i,cl}$) lie respectively. The distance along X_T and Y_T axes between those newly found points and points (INIT_X_i, INIT_Y_i) are computed using (10)-(13).

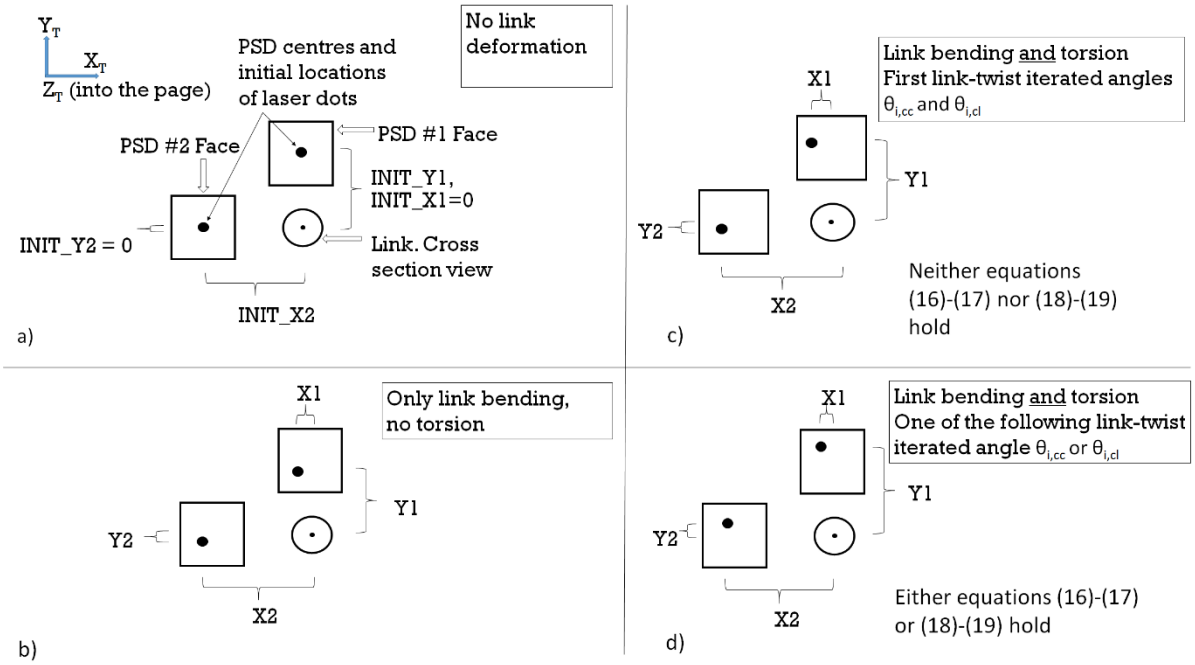

Fig. 4. a) PSD and beam before deformation, b) after bending without torsion c) after bending and torsion- iterated twist angle is incorrect, d) after bending and torsion- iterated twist angle is correct

$$\Delta X_{i,cl} = INIT\_X_i - X_{i,cl} \quad (10)$$
$$\Delta Y_{i,cl} = INIT\_Y_i - Y_{i,cl} \quad (11)$$
$$\Delta X_{i,cc} = INIT\_X_i - X_{i,cc} \quad (12)$$
$$\Delta Y_{i,cc} = INIT\_Y_i - Y_{i,cc} \quad (13)$$

For clockwise rotation, equations (1)-(4), (10) and (11) will give,

$$\begin{bmatrix}\Delta X_{i,cl}\\ \Delta Y_{i,cl}\end{bmatrix} = \begin{bmatrix}H_i + Px_{i,0}\\ V_i + Py_{i,0}\end{bmatrix} - \\ - \begin{bmatrix}\cos\theta_{i,cl} & \sin\theta_{i,cl}\\ -\sin\theta_{i,cl} & \cos\theta_{i,cl}\end{bmatrix}\begin{bmatrix}H_i + Px_i\\ V_i + Py_i\end{bmatrix} \quad (14)$$

and for counter-clockwise, equations (1)-(4), (12) and (13) will give,

$$\begin{bmatrix}\Delta X_{i,cc}\\ \Delta Y_{i,cc}\end{bmatrix} = \begin{bmatrix}H_i + Px_{i,0}\\ V_i + Py_{i,0}\end{bmatrix} - \\ - \begin{bmatrix}\cos\theta_{i,cc} & -\sin\theta_{i,cc}\\ \sin\theta_{i,cc} & \cos\theta_{i,cc}\end{bmatrix}\begin{bmatrix}H_i + Px_i\\ V_i + Py_i\end{bmatrix} \quad (15)$$

Comparison is done between the $\Delta X_{i,cl}$, $\Delta Y_{i,cl}$, $\Delta X_{i,cc}$ and $\Delta Y_{i,cc}$ calculated for each PSD.

$$(\Delta X_{1,cl}) - (\Delta X_{2,cl}) < Arbitrary\ tolerance \quad (16)$$

and

$$(\Delta Y_{1,cl}) - (\Delta Y_{2,cl}) < Arbitrary\ tolerance \quad (17)$$

or

$$(\Delta X_{1,cc}) - (\Delta X_{2,cc}) < Arbitrary\ tolerance \quad (18)$$

and

$$(\Delta Y_{1,cc}) - (\Delta Y_{2,cc}) < Arbitrary\ tolerance \quad (19)$$

If there is a match between corresponding ΔX and ΔY pairs of values (meaning either pair (16)-(17) or (18)-(19) holds), it means that the angle θ_i used in this iteration is the true torsion angle and thus ΔX_i and ΔY_i given by (14) or (15) are the magnitudes of tip deflection along X_T and Y_T axes. Equations (16) - (19) implement an arbitrary tolerance to within which the compared values from both PSDs have to be similar to each other.

If, at selected $\theta_{i,cc}$ and $\theta_{i,cl}$ neither of the above inequalities holds (Fig. 4c) , both angles have to be systematically changed at arbitrary increment of degrees and equations (14)-(15) recalculated with fresh values until a pair of them does hold (Fig. 4d).

2.2 Error sources analysis

One of the error sources is the fact that the link rotation around the global X_T and Y_T axes is ignored. This rotation would cause the X_T-Y_T plane not being perpendicular to the incoming laser beams. The greater the load on the link the more tilt the X_T-Y_T plane will have relative to X_F-Y_F.

Another source of error would be in the iteration of the angle of link's twist. The basic idea is that the iterations stop and the twist angle is determined when ΔX_1 and ΔY_1 are equal to ΔX_2 and ΔY_2, respectively.

However, in the actual computer code a small tolerance is given to how close the deflection values for the two PSDs can be, to be considered equal. This tolerance was created to prevent infinite iteration loops when the values of ΔX_1 and ΔX_2, and ΔY_1 and ΔY_2 are not respectively equal exactly. However, it may cause deformation computation error, proportional to the magnitude of the specified tolerance.

An important requirement to avoid unnecessary measurement errors is that the lasers generating the dots on PSDs be rigidly attached to an area on the setup where no bending occurs. Any dislocation of the lasers from their initial positions when INIT values were taken, will cause deflection results to appear larger or smaller than they truly are.

3 Experiment and Results

3.1 Experimental setup

The used equipment to obtain the measurements were a pair of PSDs, with photosensitive surface dimensions of 10 x 10 mm, each with its individual laser diode (rated at <1 mW), a pipe to simulate a link, and a set of weights to generate load. Since both PSDs would not fit inside the link, all the electronics were located on the outside, rigidly secured to it. PSD #1 is located directly above the link with the sensor's center located on a line parallel to Y_T axis, Fig. 5. PSD #2 is mounted directly to the side of the link with this sensor's centre located on a line parallel to X_T. The hollow link used is of constant diameter as seen in Fig. 6 along with weight application location.

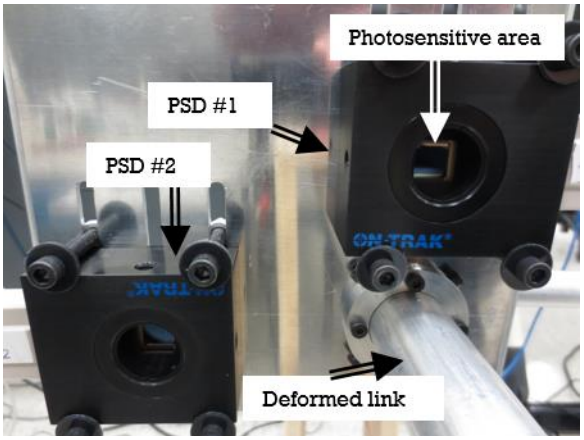

Fig. 5. Close-up of the two PSDs used in experiment

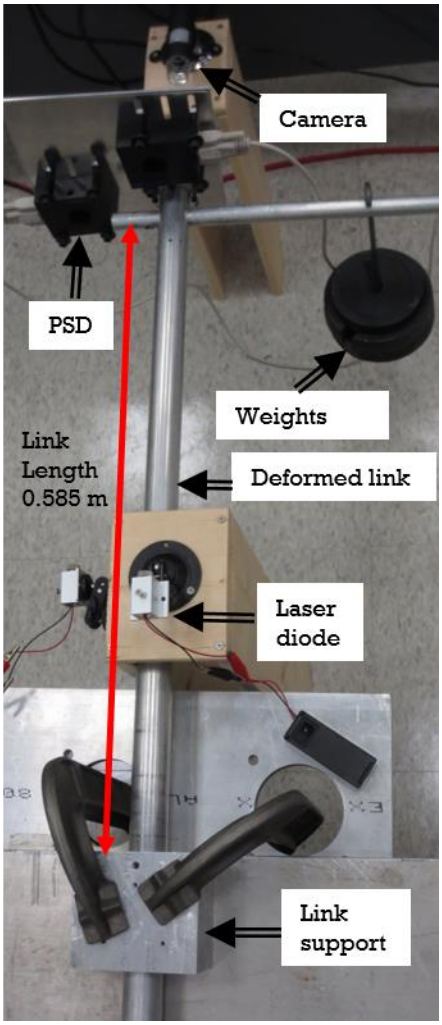

Fig. 6. Experimental setup for PSD method

The experiment consisted of starting a Simulink simulation containing the data collecting and computation modeling, while the link was not under external load (except the downward gravity force).

Applying force to the tip of the link was accomplished by hanging weights on the link's sidebar. The external weight forces used were 30 N and 50 N. This has caused the link to both bend and rotate. The movement of PSDs relative to the stationary laser beams caused the PSDs to register dot movement as electric current. The current signal was passed on to a voltage generating amplifier from where it was transferred to a computer which conducted all the iterations and calculations, plotting the deformation values in real time. Signal noise effects were reduced by averaging 20 incoming signals, and performing calculations using those average values. The system's sampling time is 1 ms, so a new value of deformation was available every 0.02 seconds.

3.2 Deflection measurement methodology comparison

To evaluate the experimental results, another method was employed to double-check the deformation values. A small paper target with three white circles on black background was rigidly attached to the deflecting tip of the link (Fig. 7). A digital camera was placed to have all three circles in its field of view and at a distance directly in front of the target to keep all circles in view during the entire experiment. The camera was decoupled from the link.

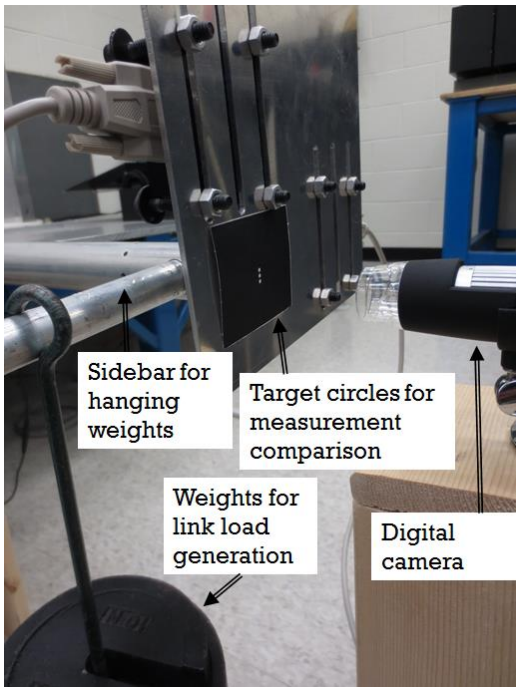

Fig. 7. Location of paper target and camera

Whenever the camera would take a picture of the target, it would break it down into pixels and process them using Matlab/Simulink model. Simulink's "Blob Analysis" block was used to identify the aforementioned three individual circles. Data obtained about these circles included circles' centroid coordinates in terms of pixel coordinate for the camera's view frame. The centroids of the top and bottom circles (Fig. 8) were used to directly determine the angle of twist of the target and therefore the link tip:

$$Link's\ Angle\ of\ Twist = \\ = tan^{-1}\left(\frac{y_{Bottom\ Centroid} - y_{Top\ Centroid}}{x_{Bottom\ Centroid} - x_{Top\ Centroid}}\right) \qquad (18)$$

The vertical and horizontal translation of the link tip were determined from the movement of the middle circle's centroid, which coincided with link's cross-section centre.

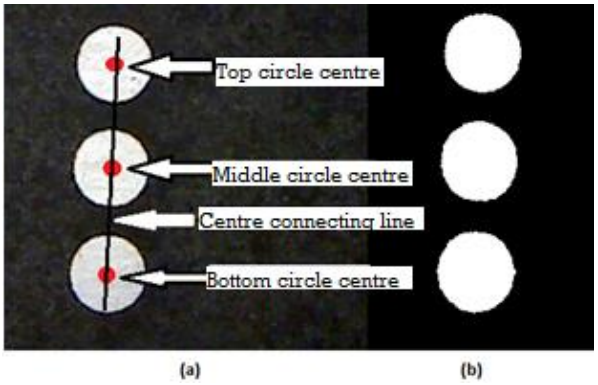

Fig. 8. Close-up of three circles used for visual link deformation magnitude confirmation; a) in color, b) Simulink's blob analysis applied

3.3 Experimental results

Tables 1 and 2 list the results from a simultaneous run of the PSD and the camera-based measurement systems. Listed are the measured link tip horizontal deflection ΔX, vertical deflection ΔY, and tip rotation angle θ.

Table 1. Results of 30 N force applied down on sidebar

Distance from link to applied force (m)	System	ΔX (mm)	ΔY (mm)	Θ (deg)
0.1	PSD	0.028	-2.140	0.030
	Camera	0.006	-2.140	0.010
0.2	PSD	0.062	-2.150	0.126
	Camera	0.002	-2.165	0.105
0.4	PSD	0.110	-2.151	0.330
	Camera	0.033	-2.185	0.346

Table 2. Results of 50 N force applied down on sidebar

Distance from link to applied force (m)	System	ΔX (mm)	ΔY (mm)	Θ (deg)
0.1	PSD	0.015	-3.443	0.083
	Camera	0.011	-3.458	0.080
0.2	PSD	0.052	-3.524	0.240
	Camera	0.022	-3.555	0.237
0.4	PSD	0.121	-3.532	0.590
	Camera	0.069	-3.590	0.595

It can be seen from the result tables that the measured deflection (ΔY) parallel to the force application direction and rotation angle θ are very similar for both methods. The deflection (ΔX) perpendicular to force application direction has discrepancy between the two methods. With used camera resolution of 640x480 pixels, the circles radius was 43 pixels and discrepancy of around 0.07 mm translates to around 3 pixels. This is due to the X and Y axes of PSDs being not precisely placed in parallel to the corresponding tip frame axes.

4 Conclusions

This paper has presented a method that is developed to determine robotic link deformation due to inertial and applied loads using installable optoelectronic modules. Two PSDs and two lasers are used to obtain required data for geometric calculations. Link bending and torsion magnitudes were obtained using the proposed method as demonstrated with experimental results. Sources of error were discussed. The next steps would be to examine a methodology which would allow the compensation for sensor plane tilting, possible with angle iterations and two PSDs, and then use position data obtained over a period of time to determine the end-effector's velocity and/or acceleration.

Acknowledgment

This work is supported in part by research grants from the Natural Sciences and Engineering Research Council of Canada (NSERC), and in part by the Canada Research Chair program.

References

[1] R. Franke, F. Hoffmann and T. Bertram. "Observation of link deformations of a robotic manipulator with fiber Bragg grating sensors", Proceedings of the 2008 IEEE/ASME Int. Conf. on Advanced Intelligent Mechatronics, Xi'an, China, 2008.

[2] J. Malzahn, A. S. Phung, F. Hoffmann and T. Bertram. "Vibration control of a multi-flexible-link robot arm under gravity", Proceedings of the 2011 IEEE Int. Conf. on Robotics and Biomimetics, Phuket, Thailand, 2011.

[3] G. Min and J.Piedbœuf. "A flexible-arm as manipulator position and force detection unit", Control Engineering Practice, 2003, vol. 11, no. 12, pp. 1433-1448.

[4] X. Wang, R. G. Langlois and M. J. D. Hayes. "Dynamic analysis of a flexible beam undergoing reciprocating rotational motion", CSME 2004 Forum.

[5] F. Demeester and H. Van Brussel. "Real-time optical measurement of robot structural deflection", Mechatronics, 1991, vol. 1, no.1, pp. 73-86.

[6] J. Swevers, D. Torfs, F. Demeester and H. Van Brussel. "Fast and accurate tracking control of a

flexible one-link robot based on real-time link deflection measurements", Mechatronics, 1992, vol. 2, no. 1, pp. 29-41.

[7] W. Yim, J. Zuang and S. N. Singh. "Experimental dual-mode control of a flexible robotic arm", Robotica, 1992, vol. 10, pp. 134-145.

[8] M. Vrhovec, I. Kovač and M. Munih. "Measurement and compensation of deformations in coordinate measurement arm", Proceedings of 2010 International Symposium on Optomechatronic Technologies (ISOT), 2010, pp.1-6.

[9] M. Vrhovec and Munih. "Improvement of coordinate measuring arm accuracy", Proceedings of IROS 2007 IEEE/RSJ Int. Conf. on Intelligent Robots and Systems, 29 Oct- 2 Nov 2007, pp. 697-702.

[10] W. L. Xu, S. K. Tso and X. S. Wang. "Conceptual design of an integrated laser-optical measuring system for flexible manipulator", Proceedings of 1996 IEEE Int. Conf. on Systems, Man, and Cybernetics, 14-17 Oct 1996, vol.2, pp.1247-1252,.

[11] T. W. Yang, W. L. Xu and S. K. Tso. "Dynamic modeling based on real-time deflection measurement and compensation control for flexible multi-link manipulators", Dynamics and Control, 2001, vol. 11, no. 1, pp. 5-24.

[12] W. L. Xu, S.K. Tso, X.S. Wang and J.Z. Zhang. "Sensor-based deflection modeling and compensation control of a flexible robotic manipulator", Proceedings of 1997 IEEE Int. Conf. on Systems, Man, and Cybernetics. Computational Cybernetics and Simulation, 12-15 Oct 1997, vol.4, pp. 3780-3785.